Building and Environment 188 (2021) 107455

Contents lists available at ScienceDirect

Building and Environment

journal homepage: http://www.elsevier.com/locate/buildenv

Modeling the similarity and the potential of toluene and moisture buffering capacities of hemp concrete on IAQ and thermal comfort

Anh Dung Tran Le [a,*], Jianshun S. Zhang [b], Zhenlei Liu [b], Driss Samri [c], Thierry Langlet [a]

[a] Laboratoire des Technologies Innovantes, EA 3899 – Université de Picardie Jules Verne, IUT Amiens, Avenue des Facultés, Le Bailly, 80025, Amiens Cedex 1, France
[b] Department of Mechanical and Aerospace Engineering, Syracuse University, 263 Link Hall, Syracuse University, Syracuse, NY, 13244, USA
[c] Centre Scientifique et Technique du Bâtiment (CSTB), 24 Rue Joseph Fourier, 38400, Saint-Martin-D'Hères, France

ARTICLE INFO

Keywords:
Hemp concrete
Toluene buffering capacity
Moisture buffering capacity
Similarity
Indoor air quality
Modeling
VOC
Moisture

ABSTRACT

Controlling and understanding indoor humidity and pollutants can help reduce the risk of health concerns. The experimental results suggested that there is a similarity relationship between water vapor and Volatile Organic Compounds (VOC) in diffusion through porous media. In this paper, the similarity between the moisture and pollutant transport and storage coefficients of porous building materials has been clearly established and explained. In addition, two similarity coefficients have been defined for VOC storage and diffusion to estimate the VOC properties from the moisture properties of the same material. A coupled hygric-pollutant (VOC) model which can be used to simulate VOC and hygric behavior of building materials under dynamic conditions is presented. The model which is implemented in the environment SPARK (Simulation Problem Analysis and Research Kernel) suited to complex problems using finite difference technique with an implicit scheme, has been validated with the experimental data. It is then applied to study the effect of toluene and moisture buffering capacities of a hemp concrete wall on indoor toluene concentration and relative humidity (RH). Hemp concrete was chosen in this study because it is an environmentally-friendly material that is used more and more in building construction. The toluene (TOL, selected VOC for this study) transport and storage properties obtained from hygrique properties of hemp concrete based on the assumption of the similarity between toluene and moisture transport have been modelled and investigated. At the room level, the results obtained show that taking into account the sorption capacity toward moisture and toluene has a significant effect on indoor RH and IAQ because hemp concrete contributes to dampen indoor RH and toluene variations. The numerical model presented is very useful for the building design optimization and can be used for a fast estimation of indoor pollution and hygrothermal conditions in building.

1. Introduction

The means for keeping the indoor relative humidity (RH) and pollutant concentration below a threshold level of interests are necessary and essential to improving building performance in terms of indoor air quality (IAQ), energy performance and durability of building materials. For evaluating the indoor air quality and thermal comfort, concentrations of pollutants such as VOC, indoor temperature and relative humidity in building are the most important factors. It has been shown that one of passive ways to keep the variation in RH between threshold levels in order to save energy and improve the thermal comfort is the use of the moisture buffering capacity of materials (including the building envelope as well as interior objects) [1–6,53,54,64],. The reduction of indoor VOC through adsorption processes is an important research objective due to its potential to provide improved quality of life for individuals in exposed spaces [7,8,55]. Formaldehyde sorption/desorption process of gypsum boards has been carried out in [56] and showed it has a significant storage capacity and influences significantly the formaldehyde concentration. The experimental data and semi-empirical models describing the sorption of organic gases in a simulated indoor residential environment (a 50 m^3 room finished with painted wallboard, carpet and cushion, draperies and furnishings) have been carried out in [57]. The results showed that the sorption appears to be a relevant indoor process and that sorption processes on typical residential surfaces can influence gas-phase concentrations on the same scale as ventilation. The contributions from several consumer goods and

* Corresponding author.
E-mail address: anh.dung.tran.le@u-picardie.fr (A.D. Tran Le).

https://doi.org/10.1016/j.buildenv.2020.107455
Received 21 August 2020; Received in revised form 21 October 2020; Accepted 7 November 2020
Available online 12 November 2020

building materials (gypsum board, ceiling tiles, furniture and carpet) to the overall formaldehyde concentration were investigated in climate-controlled chamber experiments by Ref. [9]. The results showed that the formaldehyde concentration in real indoor air will always be influenced by multiple parameters and cannot be simply calculated from the area-specific emission rate of a building material under consideration of loading rate and air exchange rate as usually done.

The use of vegetable particles (such as hemp shives, flax shives, straw bales, etc.) as building material aggregates is an interesting solution as they are eco-friendly materials and have low embodied energy. Among these vegetable particles, hemp shives have been extensively studied in many researches [10–16]. Hemp shives can be used as particle boards, biodegradable plastics, building materials for thermal and acoustic insulation products [17], etc. Regarding the emissions of bacteria and volatile organic compounds (VOCs), the experimental results showed that they are negligible [14,18]. Hemp concrete which is one of these materials is more and more recommended by the eco-builders for its low environmental impact. The physical properties (thermal conductivity, heat capacity, sorption isotherm, water vapor permeability, etc.) of hemp concrete have been measured by many authors [19–24] showing that this material presents high moisture buffering capacity and a good compromise between insulation and inertia materials. Therefore, hemp concrete is chosen for this study. It is noted that the composition and manufacturing have a significant impact on hygrothermal properties and anisotropie of hemp concrete [25–28]. Up to date, most studies focus on hygrothermal behavior and mechanical performance of bio-based materials [58]. Although the study of pollutant behavior (VOCs) of bio-based materials is very important as the building materials represent an important part of indoor environments (hygrothermal comfort and IAQ).

Regarding volatile organic compound (VOC), the experimental studies showed that there is a similarity between moisture and VOC diffusion through porous media [29–31]. Note that the diffusion and sorption of VOC and water vapor in building materials would be related to physical and chemical properties. The results obtained in[31] showed that the VOC diffusivity in air at reference temperature varies with the molar mass of the VOC and the heavier VOC has a lower diffusivity in free air than the one of water vapor. The study in [8] showed that the adsorption/desorption characteristics are related to material microstructure and polarity of the VOCs. Therefore, the difference in physical properties (size, molar mass, polarity, etc.) would play a role in the similar behavior between VOCs and water vapor which needs to be further investigated. The tests with gypsum wallboard, oriented strand board and silicate calcium using a dual chamber experimental system showed this similarity can be used to estimate the VOC diffusion coefficient if the water vapor diffusivity is known for the same material based on the conventional dry cup method [29,30]. Compared to the previous study of [30]; the similarities between VOC and moisture transport in building materials have been extended for non-isothermal problems in the framework of Annex 68 [31]. The experimental results obtained by Ref. [9] have revealed that the formaldehyde concentration in real indoor air can only be explained accurately when taking into account multiple parameters such as adsorption/desorption as well as diffusion inside material.

The literature review showed that there is lack of a comprehensible and validated model to study the hygric and pollutant behavior of bio-based materials. Therefore, to address this lack, a coupled hygric and VOC transport simulation model has been presented and validated in this paper. In addition, the purpose of this paper is to model the similarities between VOC and moisture transport properties and to show the potential of VOC and moisture buffering capacity of hemp concrete to improve IAQ and thermal comfort. The potential of buffering capacity of hygroscopic material can be explained by the fact they can adsorb VOC/moisture from the ambient air when the indoor VOC/humidity increases, and release VOC/moisture to the ambient air when the VOC/humidity decreases.The toluene (TOL) was selected as reference VOCs in this study because it is a typical indoor VOC and not water soluble.

2. Coupled moisture, air and pollutant transport model

A coupled hygric and pollutant simulation model presented in Fig. 1 has been developed to study the similarity between moisture and pollutant behavior of porous building materials. The model includes equations that describe: moisture and VOC diffusion, moisture and VOC sorption, impact of RH and T on moisture and VOC diffusion/sorption, boundary condition between indoor/outdoor air and building envelope surfaces, etc. In this section, the similarity between the moisture and VOC transport and storage coefficients of building materials will be established and explained based on the following accepted assumptions:

- Transport of water vapor in building materials is modelled analogously to the transport of VOC.
- Sorption of water vapor is described by the sorption isotherm curve (due to its multilayer adsorption) while it is modelled by the partition coefficient for VOC because it is generally considered as monolayer adsorption.

2.1. Similarity of pollutants and moisture transport models

In this article, the VOC and moisture diffusion models which take into account the effect of moisture content/RH in building materials on VOC transport are presented. To establish the similarity between the VOC and moisture diffusion models, only concentration gradient of VOC or moisture is assumed to be driving force in the material. It is important to note that the chemical reactions are neglected in this work.

For a dry material with homogeneous diffusivity, the VOC mass transport within the wall can be described by the one-dimensional diffusion [32–34]:

$$\frac{\partial C_{m,VOC}}{\partial t} = \frac{\partial}{\partial x}\left(D_{m,VOC}\frac{\partial C_{m,VOC}}{\partial x}\right) \quad (1)$$

Where $C_{m,VOC}$ is VOC concentration in the material (kg/m^3), $D_{m,VOC}$ is diffusion coefficient of the VOC in the material (m^2/s), x is abscissa (m) and t is time (s). Here, in the developed numerical model, the $D_{m,VOC}$ is a function of relative humidity/moisture in the material (if the data is available) while the dependence of $D_{m,VOC}$ on pollutants concentration is neglected as generally accepted under low VOC concentration condition.

There is an equilibrium which exists between the concentration of VOC in a material ($C_{m,VOC}$) and the concentration in air ($C_{a,VOC}$), which is defined by the partition coefficient $K_{m,VOC}$:

$$C_{m,VOC} = K_{m,VOC}.C_{a,VOC} \quad (2)$$

The diffusion coefficient of VOC in the material ($D_{m,VOC}$) can be determined from the VOC diffusion coefficient in the free air (D_{VOC}^{air}) and diffusion resistance factor (μ_{VOC}) of VOC [30]:

$$D_{m,VOC} = \frac{D_{VOC}^{air}}{\mu_{VOC}K_{m,VOC}} \quad (3)$$

At the material-air interface, we assume an instantaneous equilibrium between VOC concentration (kg/m^3) in the air near material surface ($C_{a,VOC,s}$) and the one in the surface layer ($C_{m,VOC,s}$):

$$C_{m,VOC,s} = K_{m,VOC}.C_{a,VOC,s} \quad (4)$$

With the following boundary conditions applied respectively for the external (x = 0) and internal (x = L) surfaces of the wall:

$$-\left(D_{m,VOC}\frac{\partial C_{m,VOC}}{\partial x}\right)_{x=0,e} = h_{m,VOC,e}\left(C_{a,VOC,e} - C_{a,VOC,s,e}\right) \quad (5)$$

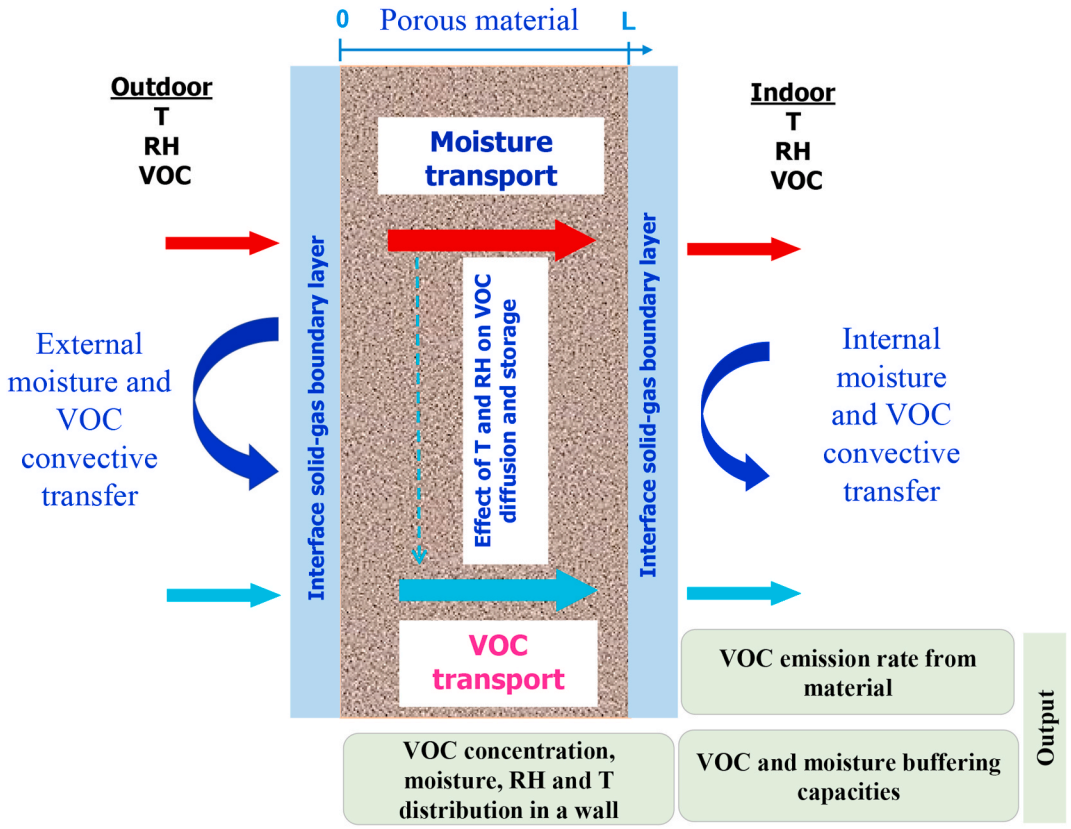

Fig. 1. Schematic of coupled moisture and VOC transport model in a wall.

$$-\left(D_{m,VOC}\frac{\partial C_{m,VOC}}{\partial x}\right)_{x=L,i}=h_{m,\mathrm{VOC},i}\left(C_{a,VOC,s,i}-C_{a,\mathrm{VOC},i}\right) \tag{6}$$

Where $C_{a,VOC,i}$ and $C_{a,VOC,e}$ are VOC concentration in the room air and outside (kg/m^3); $C_{a,VOC,s,i}$ and $C_{a,VOC,s,e}$ are VOC concentrations in the air near internal and external surfaces (kg/m^3); $h_{m,VOC,e}$ and $h_{m,VOC,i}$ are convective VOC transfer coefficients (m/s) for the external and internal surfaces, respectively.

Concerning the moisture transport model, the moisture transport within the wall can be described by the one-dimensional diffusion for using moisture content in material as driving force [35]:

$$\frac{\partial\theta}{\partial t}=\frac{\partial}{\partial x}\left(D_{m,\mathrm{wv}}\frac{\partial\theta}{\partial x}\right) \tag{7}$$

Where θ is moisture volumetric content in the material (m^3 of water/m^3 of material), $D_{m,wv}$ is diffusion coefficient of the moisture in the material (m^2/s) which is defined by Ref. [35,59]:

$$D_{m,\mathrm{wv}}=\delta_{wv}\frac{P_{v,sat}}{\rho_w}\frac{1}{\partial\theta/\partial RH}=\frac{\delta_{wv}^{air}}{\mu_{wv}}\frac{P_{v,sat}}{\rho_w}\frac{1}{\partial\theta/\partial RH} \tag{8}$$

$\partial\theta/\partial RH$ is the slope of the sorption isotherm curve which designates the relationship between the moisture content and the relative humidity (RH) at a fixed temperature, δ_{wv} is water vapor permeability of material (kg/(m.s.Pa)), ρ_w is density of water (kg/m^3), $P_{v,sat}$ saturation pressure of water vapor (Pa), μ_{wv} the vapor diffusion resistance factor and δ_{wv}^{air} is water vapor permeability of still air ((kg/(m.s.Pa)) which can be determined from D_{wv}^{air} (water vapor diffusion coefficient in the free air, m^2/s), temperature and the gas constant for water vapor (R_v = 461.5 J/(kg·K)):

$$\delta_{wv}^{air}=\frac{D_{wv}^{air}}{R_vT} \tag{9}$$

By replacing (9) in (8) we have:

$$D_{m,\mathrm{wv}}=\frac{D_{wv}^{air}}{\mu_{wv}\frac{\rho_wR_vT}{P_{v,sat}}\frac{\partial\theta}{\partial RH}}=\frac{D_{wv}^{air}}{\mu_{wv}K_{m,wv}} \tag{10}$$

As with the VOC, by identifying two equations (3) and (10), the coefficient $K_{m,wv}$ introduced in (10) is the "partition coefficient" for water vapor, which is similar to $K_{m,VOC}$ in (3) for VOC and can be calculated as following:

$$K_{m,wv}=\frac{\rho_wR_vT}{P_{v,sat}}\frac{\partial\theta}{\partial RH} \tag{11}$$

Note that the partition coefficient ($K_{m,wv}$) for water vapor can be calculated by relating gradients of the absorbed moisture content mass by volume of material, to gradients of the humidity of air by volume of the pores at equilibrium condition. Using this definition to calculate $K_{m,wv}$, the same result was obtained [31].

Concerning the sorption isotherm, in this article, the Guggenheim-Anderson-deBoer (GAB) model [60] which is extended from Langmuir and BET theories [61,62] of physical adsorption, is used to describe the sorption curve. Using the GAB model has many advantages such as having a viable theoretical background and giving a good description of the sorption behavior of hygroscopic material [37]. The GAB model can be written as follows:

$$w=\frac{w_mC_{GAB}K_{GAB}RH}{(1-K_{GAB}RH)(1+K_{GAB}C_{GAB}RH-K_{GAB}RH)} \tag{12}$$

Where RH is relative humidity, w is the moisture content (kg of water/kg of material), w_m is the monolayer moisture content value, C_{GAB} and K_{GAB} are energy constants of GAB model.

At the material-air interface, we assume an instantaneous equilibrium between water vapor concentration (kg/m^3) in the air near material surface ($C_{a,wv,s}$) and the one in the surface layer ($C_{m,wv,s}$), which is determined by the sorption isotherm curve. The following boundary conditions applied to water vapor, respectively for the external (x = 0) and internal (x = L) surfaces of the wall:

$$-\left(\rho_w D_{m,wv}\frac{\partial\theta}{\partial x}\right)_{x=0,e} = h_{m,wv,e}\left(C_{a,wv,e} - C_{a,wv,s,e}\right) \quad (13)$$

$$-\left(\rho_w D_{m,wv}\frac{\partial\theta}{\partial x}\right)_{x=L,i} = h_{m,wv,i}\left(C_{a,wv,s,i} - C_{a,wv,i}\right) \quad (14)$$

Where $C_{a,wv,i}$ and $C_{a,wv,e}$ are water vapor concentrations in the room air and outside (kg/m^3), and $h_{m,wv,e}$ and $h_{m,wv,i}$ are convective water vapor transfer coefficients (m/s) for the external and internal surfaces.

The mass transfer coefficient may be measured directly or indirectly using the naphthalene sublimation technique or from published heat transfer coefficients or correlations using the so-called heat and mass transfer analogy [38]. The convection average mass transfer coefficient strongly depends upon the characteristics of the airflow at the material surface. These correlations relate the Sherwood number (Sh), to the Rayleigh (Ra) and Schmidt (Sc) numbers in the case of natural convection, and to the Reynolds (Re) and Schmidt (Sc) numbers in the case of forced convection [39]. The convective mass transfer coefficient for VOC and water vapor (WV) ($h_{m,VOC}$, $h_{m,wv}$) can be calculated by the following equations [38–40]:

$$Sh = 0.037 Sc^{\frac{1}{3}} \mathrm{Re}^{\frac{4}{5}} \text{ for turbulent flow} \quad (15)$$

$$Sh = 0.664 Sc^{\frac{1}{3}} \mathrm{Re}^{\frac{1}{2}} \text{ for laminar flow} \quad (16)$$

$$Sh = \frac{h_m L}{D^{air}} \quad (17)$$

$$Sc = \frac{\upsilon}{D^{air}} \quad (18)$$

where, Sh is Sherwood number, Sc is Schmidt number, h_m is the convective mass transfer coefficient (m/s), L is the characteristic length (m), D^{air} is diffusion coefficient of VOC/water vapor in air (m^2/s), υ is kinematic viscosity of air at 23 °C, which equals 1.544 x10^{-5} m^2/s [63]. From equations (15)–(18), we can establish the similarity relationship between $h_{m,wv}$ and $h_{m,VOC}$. Note that, because of the same sample and the same air flow field in the airtight chamber as the same test condition for the combined moisture and VOC study, the same Reynolds number can be considered, and we have the following formula:

$$\frac{h_{m,wv}}{h_{m,VOC}} = \left(\frac{D_{wv}^{air}}{D_{VOC}^{air}}\right)^{\frac{2}{3}} \quad (19)$$

Equation (19) permits to determine the convective mass transfer coefficient of VOC ($h_{m,VOC}$) from the convective mass transfer coefficient of water vapor $h_{m,wv}$ (or inversely) using the diffusion coefficients of VOC and water vapor in the air, respectively.

2.2. Model for a room

In order to model the indoor VOC and humidity in the room, we used a nodal method, which considers the room as a perfectly mixed zone characterized by a moisture and pollutant concentrations. Nodal method involves equations for moisture/pollutant (VOC) mass balance and equations describing mass transfer through the walls, additional convection between inside wall surfaces and room ambiance. The moisture/VOC level in the room is determined by the moisture/VOC transfer from interior surfaces, moisture/VOC production rate and the gains or losses due to air infiltration, natural and mechanical ventilation, sources due to habitants of room as well as the moisture/VOC buffering capacity of other room elements (such as furniture, bookshelf, woolen carpet, etc.). This yields to the following mass balance equation for water vapor/VOC:

$$V\frac{\partial C_{a,i}}{\partial t} = Q\left(C_{a,o} - C_{a,i}\right) + \sum A.h_{m,i}\left(C_{as,i} - C_{a,i}\right) + G \quad (20)$$

Where $C_{a,i}$ is the VOC/water vapor concentration at time t (kg/m^3); $C_{a,o}$ is outdoor ventilation air; V is volume space (m^3); the summation symbol represents the sum of moisture/VOC exchanged between indoor air and the exposed area of the material; A is exposed area of the material (m^2); Q is the volume air flow rate into (and out) of the room (m^3/s); G is the generation rate of VOC/water vapor in the room (kg/s).

2.3. Numerical solutions and validation

The set of equations describing the model has been solved using the finite difference technique with an implicit scheme. The Simulation Problem Analysis and Research Kernel (SPARK) developed by the Lawrence Berkeley National Laboratory-USA, a simulation environment allowing to solve efficiently differential equation systems has been used to solve this set of equations [5,41–44].

Note that the equations contain several parameters that are themselves function of the state variables. The special interests of the developed model in this paper are the dependencies of moisture transport coefficient, pollutant diffusion coefficient, partial coefficient, etc. upon the relative humidity and temperature can be taken into account if the data is available. This makes it possible to take into account of the effect of T and RH on pollutant and hygrothermal behavior of building materials into the model.

This section concerns the validation of the developed model by comparing the numerical results with experimental ones obtained using the dynamic dual chamber method developed by Ref. [30,45]. The two stainless steel chambers which have the dimension of 0.35 m × 0.35 m x 0.15 m each were partitioned by a test specimen (Fig. 2). Each chamber was supplied with inflows under controlled temperature and relative humidity. Both chambers were supplied with the same airflow rate (Q = 6.58 × 10^{-2} m^3/s) and were placed in the laboratory with constant temperature 23 °C.

Concerning the relative humidity of the inflow for both chambers, it was maintained at threshold level by bubbling the liquid water via a PID (proportional-integral-derivative) control. The temperature and relative humidity of the inflow and outflow for both chambers were recorded continuously by a computer-based data acquisition system.

Regarding VOC, chamber A had a constant VOC injection in the inflow which was supplied by a Dynacalibrator containing a VOC permeation tube maintained at a specific temperature while chamber B had no VOC injection. The VOC concentration in the inflow of chamber A was set at constant, and the concentration in chambers A and B were continuously monitored until they reached a steady state. Concentrations in the outlets of chamber A and B were monitored as C_{Aout} and C_{Bout}. Under well mixed condition, C_A=C_{Aout} and C_B=C_{Bout} and at steady state, C_{Aout} and C_{Bout} were constant. Constant VOC concentration into chamber A (C_{Ain}) was provided by the permeation tube within a dynacalibrator. VOC concentrations (toluene) of the outflows of both chambers were measured by proton transfer reaction mass spectrometry (PTRMS), which was pre-calibrated by the permeation tube under each RH condition because PTRMS measurement might be influenced by RH depending on the property of the specific VOC. Note that, RH and VOC concentration in the inflow of chamber A (C_{Ain} and RH_{Ain}), in chamber B (C_B and RH_B) are used as the input data. The relative humidity and VOC concentration in chamber A (C_A and RH_A) are used for model validation.

Calcium silicate was selected as a reference material for the model validation in this study because of its well-characterized moisture diffusion properties and wide usage as a building insulation material. Besides, calcium silicate is hygroscopic material and clean meaning that it had no VOCs added in the fabrication. The calcium silicate was cut

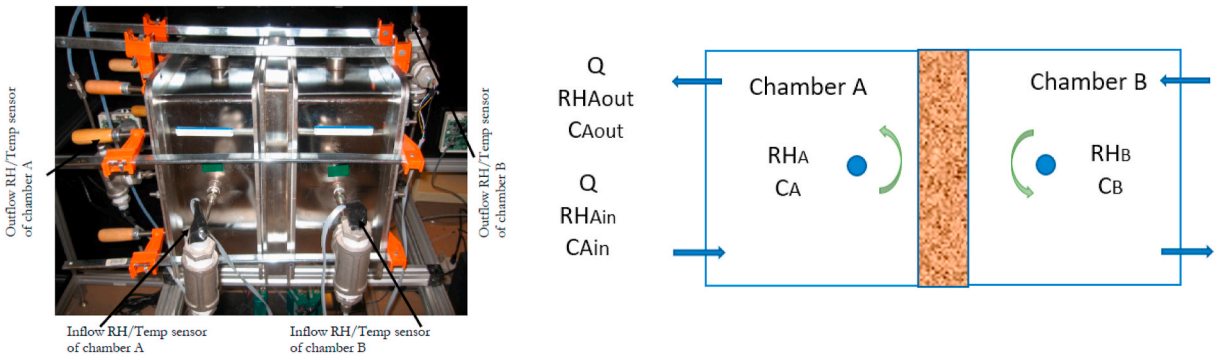

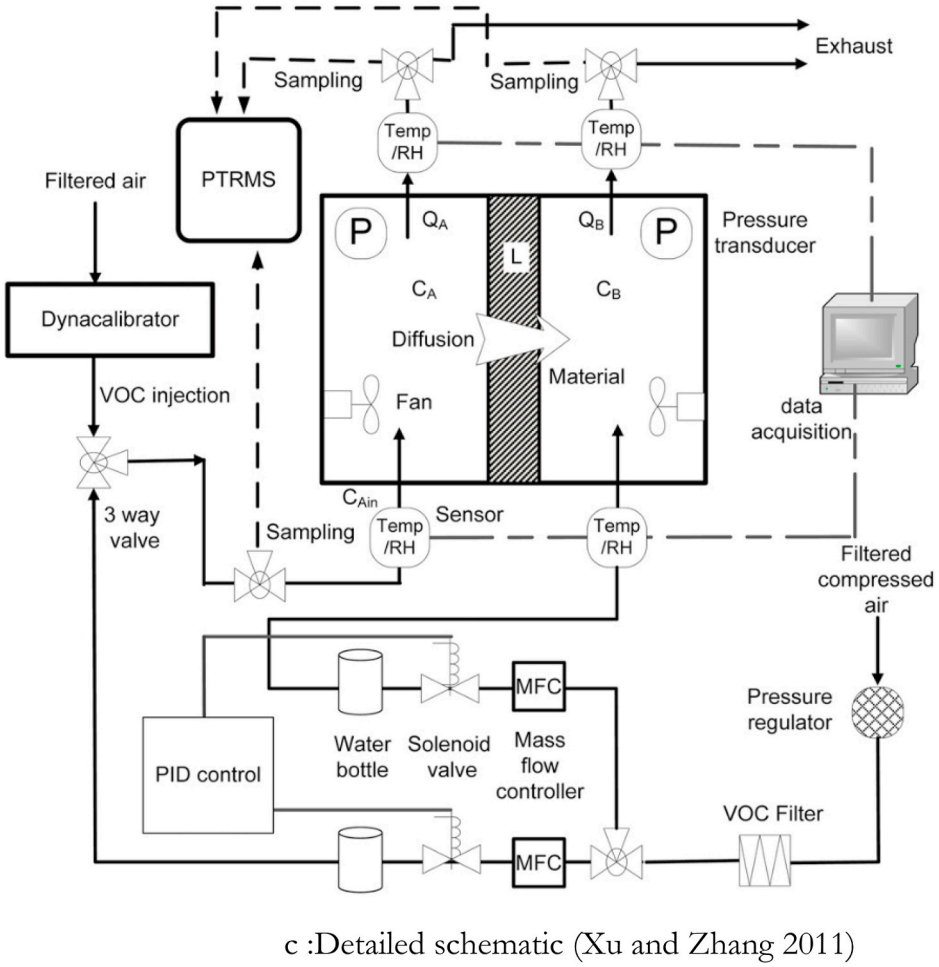

Fig. 2. Dual chamber system: photograph, detailed schematic [45] and test schematic for simulation conditions.

into a 30.5 cm × 30.5 cm x 1.0 cm, and sealed four edge sides by VOC free tape (resulted in a real exposed area of 0.093 m^2) to prevent VOC diffusion through the edges. The specimen was then placed in a specially prepared steel specimen holder between two chambers, and clamped tightly together. More information about the testing can be fund in Ref. [30,45]. In order to validate the developed models, two tests were used:

- Test for validating the VOC model: VOC concentration (toluene) has been injected (C_{Ain} = 383 μg/m^3) into chamber A while T and RH in both chambers A and B were maintained at 23 °C and 50%RH. In the meantime, VOC, RH (C_{Ain} and RH_{Ain}, C_A and RH_A, C_B and RH_B) have been recorded continuously.
- Test for validating the moisture model: the initial RHs in chamber A and B were both 50%. When the test began, the RH of inflow for chamber A was increased to 80% RH while maintaining a constant 50% RH inflow for chamber B, and the changes of RHs in chamber A and B were monitored over time.

The physical, hygrique and toluene properties of silicate calcium at 50% RH shown in Table 1 and Fig. 3 (for sorption isotherm) have been measured by Ref. [30] and were used for the model validation. Fig. 4 and Fig. 5 compare the simulating toluene concentrations and relative humidity in the chamber A. [47] The results show a good agreement between the numerical model and experimental results after the few hours for both pollutant and moisture models. Therefore, the developed model

Table 1
Physical, hygric and toluene properties of silicate calcium (SC) for toluene at 50% RH [45] and GAB model parameters proposed for SC.

ρ(kg/m^3)	μ_{wv}	μ_{TOL}	$K_{m,TOL}$	$D_{m,TOL}$ (m^2/s)	Sorption isotherm (GAB model parameters, $R^2 = 0.99$)
843.38	8.71	4.94	133	1.29×10^{-8}	$w_m = 0.002$; $C_{GAB} = 8$; $K_{GAB} = 0.97$

is satisfying to investigate the coupled hygric-pollutant (toluene) behavior of porous building materials. In the next section, the modeling toluene properties from moisture properties of hemp concrete will be presented.

3. Effect of toluene and moisture buffering capacities of hemp concrete wall on indoor relative humidity and toluene concentration

3.1. Modeling toluene properties from moisture properties of hemp concrete

An increased environmental awareness incites to the valorization of plant resources as building materials or incorporating construction processes. One of these building materials is hemp concrete, which has been used widely in the world and extensively studied in many researches. At the building level, it has been proven that the use of hemp concrete can damping the variation indoor RH thank to its moisture buffering capacity [3,53]. Hemp concrete has been selected for this study because it is more and more recommended by the eco-builders for its low environmental impact, excellent moisture buffering capacity and a good thermal insulation [3,4,19]. This article will focus on modeling toluene properties of sprayed hemp concrete which is made of hemp shiv

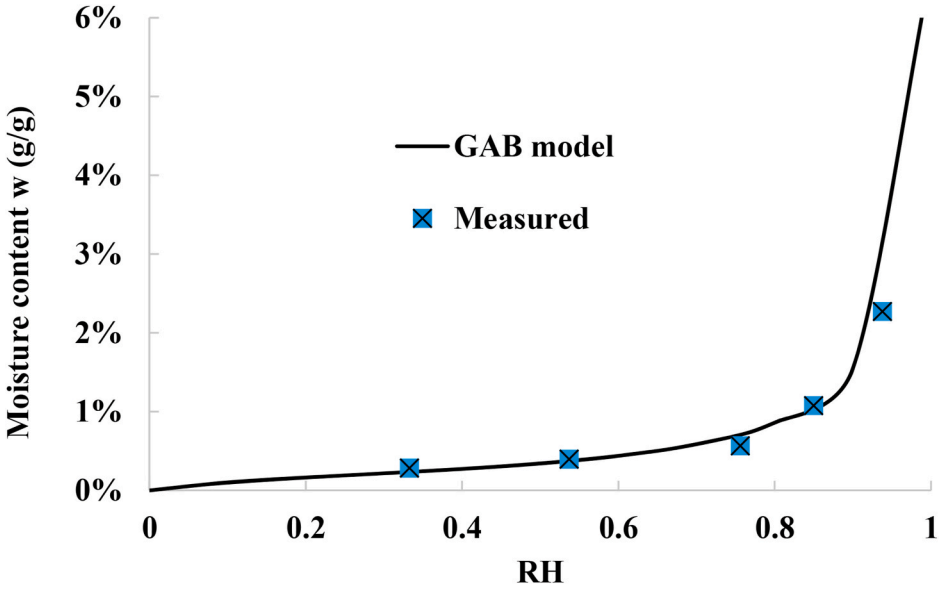

Fig. 3. Sorption isotherm of silicate calcium.

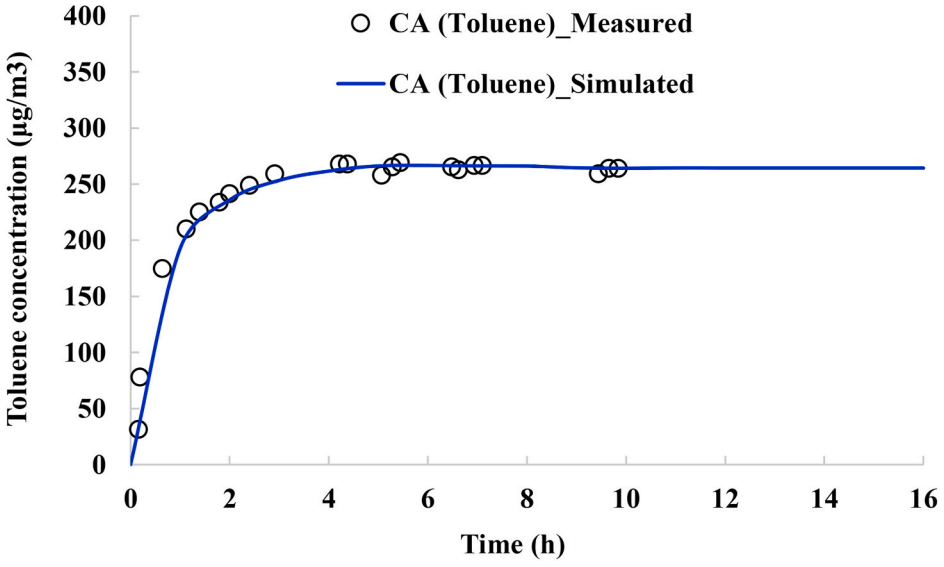

Fig. 4. Computed values and measured toluene indoor concentration in chamber A.

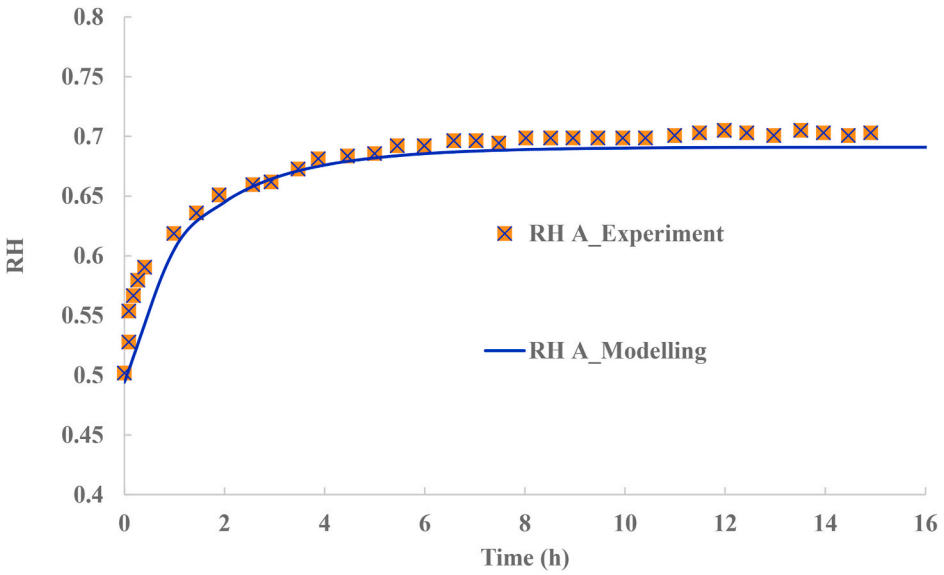

Fig. 5. Computed values and measured RH in chamber A.

mixed with Tradical PF70 binder for wall application, from the moisture properties experimentally determined in Ref. [21,23,46]. The toluene (water insoluble) which is a typical indoor VOC was selected as reference VOCs. Regarding the fact that the calculated mean free path for toluene is 14.3 nm [30] and the mean pore diameter in hemp concrete is about 780 nm [47], the molecular diffusion dominates the mechanism for toluene. Concerning water vapor, its mean free path is 100 nm [47], the molecular diffusion is predominant in hemp concrete compared to Knudsen diffusion which is also expected to occur.

Xu et al [30] proposed the similarity coefficient to correlate the pore diffusion coefficient of VOCs with that of water vapor for hygroscopic moisture conditions. The similarity coefficient for the moisture and VOC diffusion can be determined by:

$$\kappa_{\mu,VOC} = \frac{\mu_{VOC}}{\mu_{wv}} = \frac{D_{VOC}^{air}}{\mu_{wv} D_{m,\mathrm{VOC}} K_{m,VOC}} \tag{21}$$

The partition coefficient of VOC can be determined based on the vapor pressure of the compound for different materials. Based on the data obtained by Ref. [48]; the following correlation may be used when the material and compound to be studied do not match the data available [32]:

$$K_{m,VOC} = 10600 P^{-0.91} \tag{22}$$

where P is the vapor pressure of the compound in mmHg. By using equation (22) for toluene (P = 25.8 mmHg at 23 °C), the partition coefficient of toluene $K_{m,TOL}$ for hemp concrete is 550.

The similarity coefficient between toluene and water vapor ($\kappa_{\mu,TOL}$=0.56) which was experimentally determined by Ref. [30] is used to estimate the toluene diffusion coefficient for hemp concrete. Table 2 and Fig. 6 show the physical properties, vapor diffusion resistance factor and adsorption isotherm of hemp concrete obtained by other authors [21,23,46]. The results show that hemp concrete is a very porous and hygroscopic material. The calculated values of $\mu_{m,TOL}$ and $D_{m,TOL}$ by equation (21) are shown in Table 3.

Table 2
Hygric properties of hemp concrete to model toluene properties.

Dry density (kg/m^3)	Total porosity (%)	Open porosity (%)	μ_{wv}	Sorption isotherm (GAB model parameters)
450	78	66	5	$w_m = 0.02$; $C_{GAB} = 7$; $K_{GAB} = 0.89$

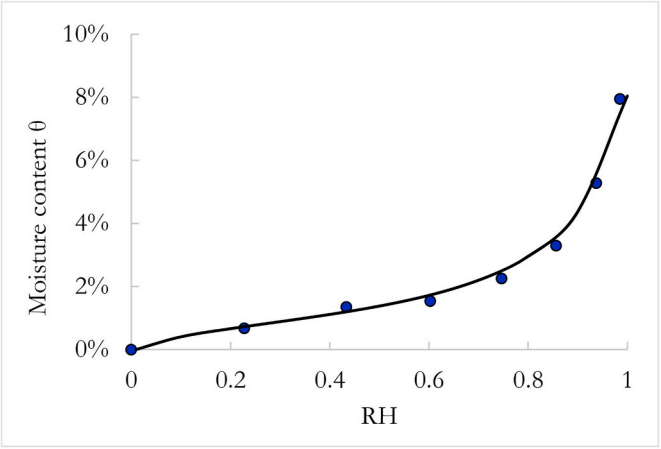

Fig. 6. Sorption isotherm of hemp concrete.

Concerning the partition coefficient of water vapor ($K_{m,wv}$), it is calculated by Equation (11) and the result determined at 10% RH is reported in Table 3. Equation (11) shows that $K_{m,wv}$ depends on temperature, relative humidity and the slope of the sorption isotherm of material. We can define the similarity coefficient for the moisture and VOC storage as following:

$$\kappa_{K_{m,VOC}} = \frac{K_{m,VOC}}{K_{m,wv}} \tag{23}$$

Note that it is very interesting to study the similarity ($K_{m,VOC}/K_{m,wv}$ and $\mu_{m,VOC}/\mu_{m,wv}$ for storage and diffusion properties, respectively) between VOC and moisture transport in building materials. If the similarity is justified and validated by experimental results for other pollutants, the VOC properties can be determined directly from the vapor diffusion resistance factor ($\mu_{m,wv}$) and the slope of the sorption curve in the monolayer sorption range (from 0 to 20% RH, before the beginning

Table 3
Toluene (TOL) and moisture properties of hemp concrete for the simulation.

μ_{TOL}	μ_{wv}	$K_{m,wv}$	$K_{m,TOL}$	$D_{m,TOL}$ (m^2/s)
2.8	5	1434 (at 10% RH)	550	5.5×10^{-9}

of multilayer sorption for hemp concrete case) because the VOCs sorption is generally monolayer in building materials. In this study, the calculated value of $\kappa_{K_{m,TOL}}$ for hemp concrete is 0.38 compared to 0.33 for silicate calcium obtained experimentally by Ref. [30].

3.2. Description of studied room and simulation conditions

The studied office is depicted in Fig. 7 and has a space area of 5*4 m^2 and a volume of 50 m^3. To study the impact of moisture and toluene buffering capacities of hemp concrete on the indoor RH and toluene concentration, we consider a total exposed surface area S = 25 m^2 of hemp concrete (moisture and toluene interactions between indoor air and building materials are taken into account). The hygric and pollutant properties of hemp concrete presented in Table 2, Table 3 and Fig. 6 were used for the simulation. The room temperature is constant and kept at 20 °C. The ventilation uses the external conditions in which the outdoor temperature and relative humidity are 20 °C and 50%, respectively. The room is occupied by two persons from 8.00 a.m. to 17.00 p.m. and the water vapor source is 142 g/h. The air velocity over the wall is 0.15 m/s which is a typical designed value in buidings to ensure thermal comfort of the occupants. The convective mass transfer coefficients for toluene and water vapor ($h_{m,TOL}$ and $h_{m,wv}$) were calculated by the equations 15–19.

In this article, an outdoor toluene concentration of 0 mg/m^3 and a ventilation rate of 0.72 ACH (Air Changes per Hour) determined based on the ventilation rate required in the French office buildings are considered. The hemp concrete wall has a thickness of 20 cm and is divided into 25 nodes. The time step is 240s. The only interaction (moisture/toluene) between the internal exposed surface of hemp concrete wall and indoor air is taken into account and the other faces of the material are considered "well sealed". The initial relative humidity is 60% RH and the initial toluene concentrations C_0 in hemp concrete is 0 (μg/m^3) because it is considered as a clean material. To study the effect of toluene buffering capacity of hemp concrete, a toluene source scheme following is considered: 12 h of 1000 μg/h followed intermittently 12 h of 0 μg/h.

In this paper, two models have been considered:

- **Model with buffering capacity (BC** model**)**: Simulation taking into account the moisture and toluene sorption capacities.
- **Model without buffering capacity (Without-BC** model**)**: Simulation neglecting the moisture and toluene sorption capacities.

3.3. Results and discussion

3.3.1. Impact of toluene and moisture buffering capacities of hemp concrete wall on indoor RH and toluene concentration

The simulated results of the two models with and without toluene -moisture buffering capacity are presented in Fig. 8 and Fig. 9. In addition, Table 4 presents the analysis results (indoor RH and toluene concentration) obtained from the simulation when the equilibrium state is reached. Fig. 8showed a significant effect of the toluene buffering capacity of hemp concrete on indoor toluene variation. We define a parameter called "*peak reduced factor-PRF*" which is calculated from the indoor concentration with and without buffering capacity (C_0 corresponds to the case without buffering capacity):

$$PRF = \frac{C_0 - C}{C_0} \tag{24}$$

The PRF_{VOC} value allows to quantify the VOC buffering capacity of building materials. Regarding the values of indoor pollutant concentration at the equilibrium state, the maximum values of **BC** and **Without-BC** models are 23.6 and 27.8 μg/m^3, respectively (Table 4) (so a PRF_{TOL} of 15%). Note that PRF_{TOL} value depends on the exposure time. From IAQ analysis and design point of view, it is very interesting to define a parameter that takes into account the concentration reduction and exposure time. Thus, we define an index called "Cumulative Exposure Reduction Factor, ERFc" (unity is %.h)" which is calculated by:

$$\mathrm{ERFc} = \int_0^t PRF dt \tag{25}$$

The ERFc for toluene is 210.5% for 12 h exposure in this study. The results reveal that taking into account the toluene sorption capacity in the simulation results in damping the peak of indoor toluene concentration and thus contributes to ameliorate the indoor air quality. Concerning the variation of the indoor relative humidity, it is presented in Fig. 9 and Table 4. The results show that the moisture buffering capacity of hemp concrete allows to dampen the indoor relative humidity variation. Numerically, at the equilibrium state, the maximum indoor RH values decrease from 72.5% to 66.3% RH (a difference of 6.2% RH and PRF_{RH} = 8.6%) for **Without-BC** and **BC** models, respectively. For indoor humidity, we define a parameter called "*amplitude reduced factor-RF_a*" which is calculated from the amplitude of indoor relative humidity variation with and without moisture buffering capacity (A_0 corresponds to the case without moisture capacity):

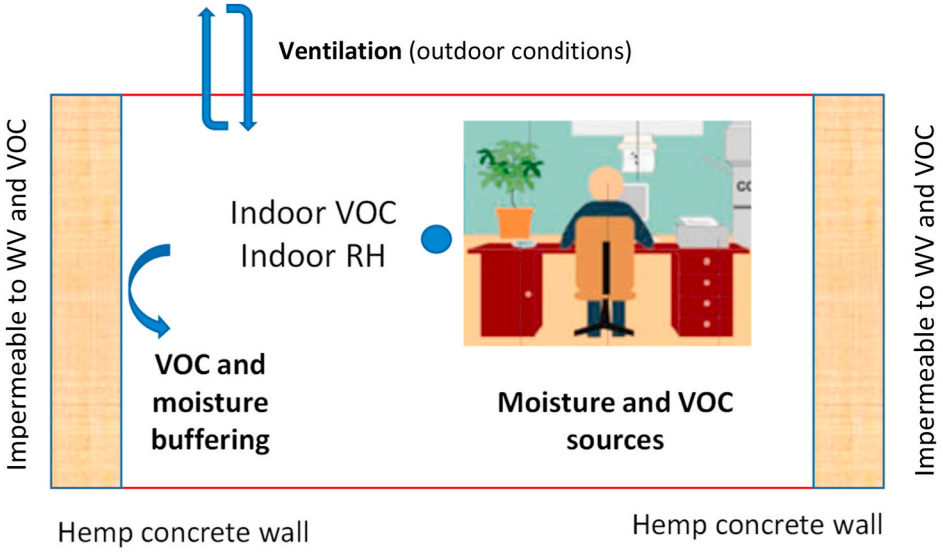

Fig. 7. Studied configuration.

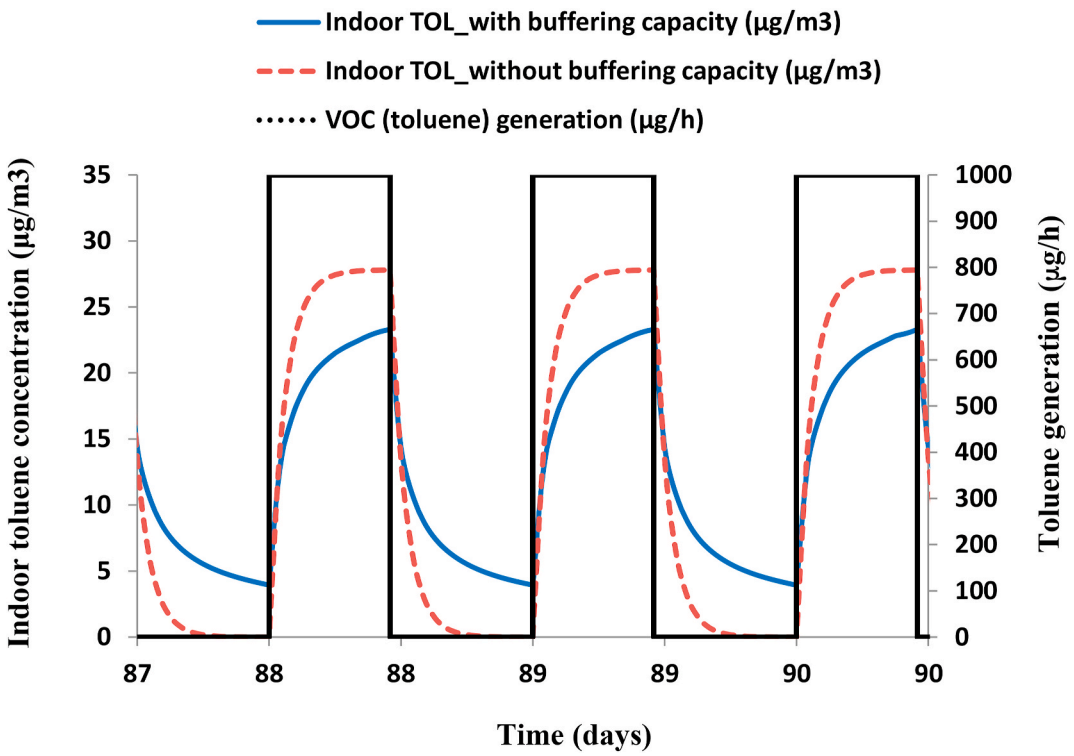

Fig. 8. Effect of toluene (TOL) sorption capacity of hemp concrete on indoor toluene concentration.

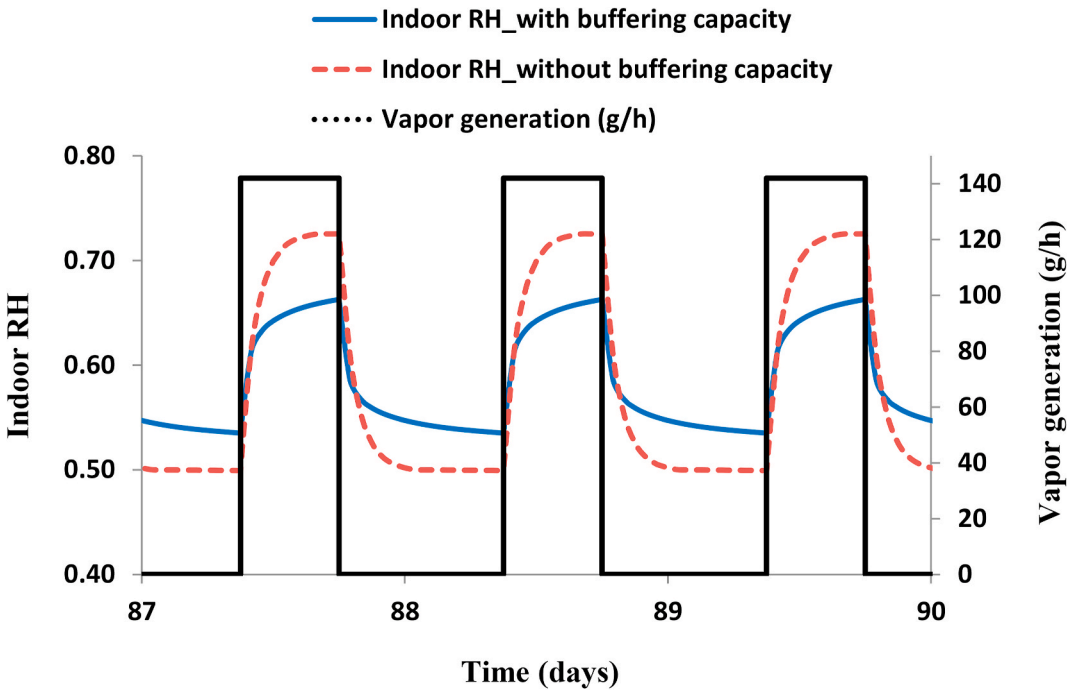

Fig. 9. Effect of moisture sorption capacity of hemp concrete on indoor RH.

$$RF_a = \frac{A_0 - A}{A_0} \quad (26)$$

The RF_a value allows to quantify the hygric buffering capacity of building materials. In addition, the RF_a value of 43.4% is obtained at peak concentration showing that taking moisture buffering capacity into account can reduce the indoor RH variation amplitude by 43.4%.

3.3.2. *Influence of $D_{m,VOC}$ and $K_{m,VOC}$ on toluene buffering capacity of hemp concrete*

It is very important to understand the influences of two key parameters $D_{m,TOL}$ and $K_{m,TOL}$, which have been modelled based on the similarity between toluene and water vapor diffusion in porous material on toluene behavior of hemp concrete. Therefore, a sensibility study of toluene buffering capacity of hemp concrete to its toluene properties has been carried out. In this part, the impact of each individual parameter

Table 4
Effect of toluene and moisture buffering capacities of hemp concrete on indoor toluene concentration and RH calculated at the equilibrium state.

	Indoor Toluene (μg/m^3)			Indoor RH (%)		
	TOL min	TOL max	Amplitude	RH min	RH max	Amplitude
BC model	3.2	23.6	20.4	53.5	66.3	12.8
Without-BC model	0	27.8	27.8	50	72.5	22.5

($D_{m,TOL}$ or $K_{m,TOL}$) on the resulting indoor toluene concentration parameter while all the other parameters remain the same as those of the reference case has been carried out.

To study the impact of the material-air partition coefficient ($K_{m,TOL}$), we considered the following values: 250; 550 (reference case); 1000; 2500, 5000. The numerical results are presented in Fig. 10 and Table 5 and show that $K_{m,TOL}$ has a significant effect on both the indoor toluene concentration and the decay/growth rate of the concentration curve. It can be seen that during the adsorption period, increasing the $K_{m,TOL}$ increases the toluene adsorption which is then diffuses into material and results in a slower indoor toluene concentration and a higher PRF_{TOL} and $ERF_{c,TOL}$ values. Numerically, during the adsorption period, when $K_{m,VOC}$ increases from 250 to 550 (reference case), 1000, 2500 and 5000, the PRF_{TOL} value increases from 8.8% to 15%, 19.6%, 25.6% and 30.1%, respectively (see Table 5). The observation is reversed during the desorption period.

Concerning the influence of $D_{m,TOL}$ (m^2/s), the following values have been used for the simulation: 5.5×10^{-7}; 5.5×10^{-8}; 5.5×10^{-9} (reference case); 5.5×10^{-10} and 5.5×10^{-11} (m^2/s) which have been denoted by: $100xD_{m,TOL,reference}$; $10xD_{m,TOL,reference}$; $D_{m,TOL,reference}$; $0.1xD_{m,TOL,reference}$ and $0.01xD_{m,TOL,reference}$, respectively (see Fig. 11). The numerical results presented in Fig. 11 and Table 6 show that the impact of $D_{m,TOL}$ is significant. During the adsorption period, higher $D_{m,TOL}$ results in a lower peak concentration. However, the impact of a change in $D_{m,TOL}$ is insignificant when the $D_{m,TOL}$ value is below 5.5×10^{-11} (m^2/s) or above 5.5×10^{-8} (m^2/s). Numerically, when $K_{m,TOL}$ increases from 550 to 1000 (by a factor of 1.8) the PRF_{TOL} increases from 15% to 19.6% (see Table 5) compared to a value of 22.2% when $D_{m,TOL}$ increases by a factor of 10 ($D_{m,TOL}$ increases from 5.5×10^{-9} to 5.5×10^{-8} (m^2/s)). The results suggest that the toluene buffering capacity of the SC board depends on both $K_{m,TOL}$ and $D_{m,TOL}$ but more sensitive with variation of the material-air partition coefficient ($K_{m,TOL}$).

Table 5
Impact of $K_{m,TOL}$ of hemp concrete on indoor toluene concentration, amplitude, PRF_{TOL} and $EFR_{C,TOL}$.

$K_{m,VOC}$	C_{max} (μg/m^3)	C_{min} (μg/m^3)	Amplitude (μg/m^3)	PRF_{TOL} (%)	$ERF_{c,TOL}$ (%.h)
$K_{m,VOC} = 5000$	19.4	4.6	14.8	30.1	343.0
$K_{m,VOC} = 2500$	20.7	4.9	15.8	25.6	293
$K_{m,VOC} = 1000$	22.3	4.2	18.2	19.6	246.8
$K_{m,VOC} = 550$ (reference)	***23.6***	***3.2***	***20.4***	***15.0***	***210.5***
$K_{m,VOC} = 250$	25.3	1.9	23.4	8.8	149
Without-BC model	27.8	0.0	27.8	0.0	0

3.3.3. *Impact of exposed surface area (A) and loading ratio on IAQ and indoor RH*

The moisture and VOC buffering potential of hemp concrete will be fully utilized when the material is directly exposed to indoor air. In the case that hemp concrete is rendered/plastered, the internal plaster should have impact on moisture and pollutant buffering capacity of hemp concrete and it is suggested to use the internal plaster which its moisture/VOC penetration depth is greater than their thickness in the system [49]. In addition, regarding the material selection process in building design, it is important to study the effect of exposed surface area (A parameter in equation (20)) and the loading ratio (the ratio of the wall surface area to the volume of the room) of hemp concrete on IAQ and hygric performance. Thus, the simulation has been done with different exposed surfaces from 0 to 25 m^2 (loading ratio from 0 to 0.5) with a step of 5 m^2. Fig. 12, Fig. 13, Table 7 and Table 8 show the effect of surface and the loading ratio on indoor toluene, RH and other indices defined previously. It can be seen that the impact of exposed surface (A) is significant and when the loading ration of hemp concrete is increased/decreased, the indoor toluene concentration and RH during the adsorption/desorption period is decreased/increased. Numerically, when the exposed surface decreases from 25 m^2 to 15 m^2 (loading ratio decreases from 0.5 to 0.3, so a reduction of 40%), the PRF_{TOL} decreases from 15% to 10% and the PRF_{RH} decreases from 8.6% to 6.4%,

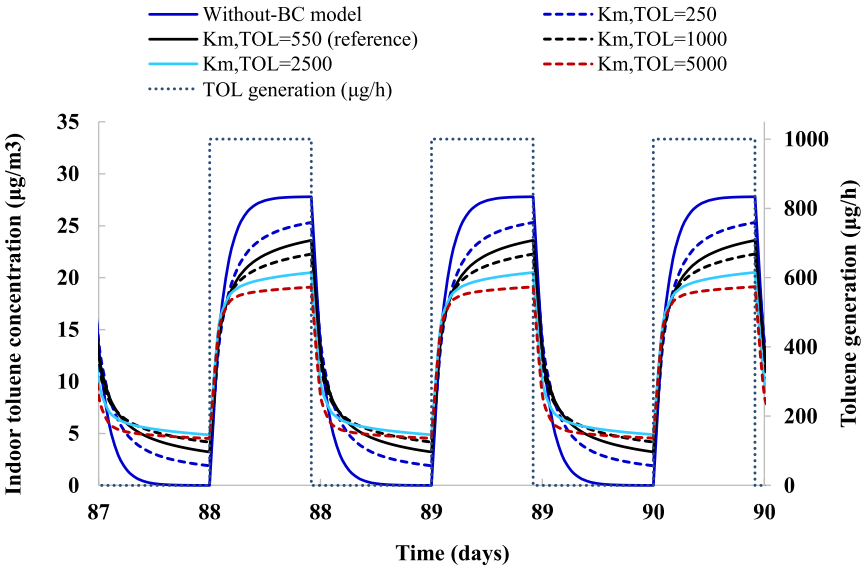

Fig. 10. Effect of $K_{m,TOL}$ of hemp concrete on indoor toluene concentration.

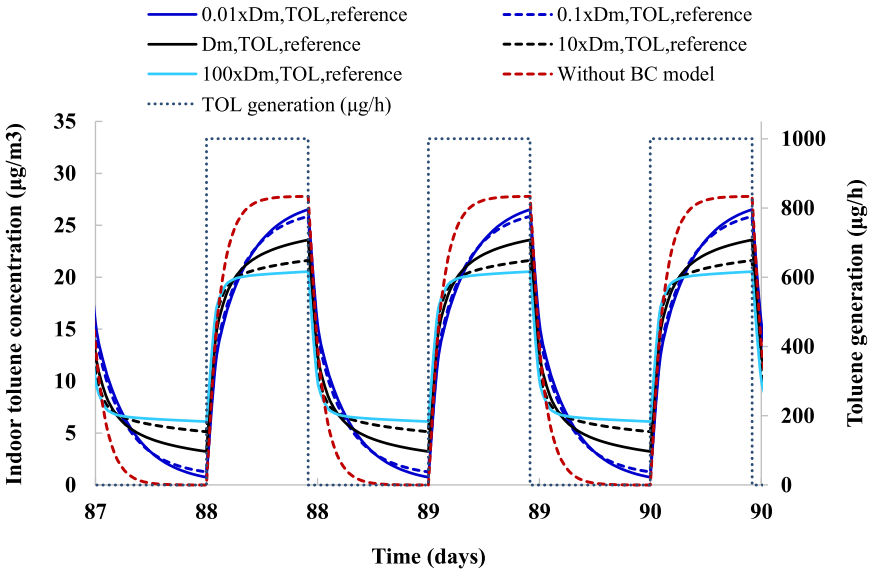

Fig. 11. Effect of $D_{m,TOL}$ of hemp concrete on indoor toluene concentration.

Table 6
Impact of $D_{m,TOL}$ of hemp concrete on indoor toluene concentration, amplitude, PRF_{TOL} and $EFR_{C,TOL}$.

Cases studied	C_{max} (µg/m^3)	C_{min} (µg/m^3)	Amplitude (µg/m^3)	PRF_{TOL} (%)	$ERF_{c,TOL}$ (%.h)
Without BC model	27.8	0.0	27.8	0.0	0.0
100x $D_{m,TOL,ref}$	20.5	6.1	14.4	26.1	271
10x $D_{m,TOL,ref}$	21.6	5.1	16.5	22.2	252
$D_{m,TOL,ref}$	***23.6***	***3.2***	***20.4***	***15.0***	***210.5***
0.1x $D_{m,TOL,ref}$	25.9	1.3	24.6	6.9	175
0.01x $D_{m,TOL,ref}$	26.5	0.7	25.8	4.6	173.9

respectively. The developed model in this paper is very useful in building design because it can be used to analyze quantitatively the effect of pollutant and moisture buffering capacity of materials which is considered as a solution to improving IAQ as well as hygrothermal performance of buildings.

4. Conclusion

In this paper, the similarity and the potential of toluene and moisture buffering capacities of hemp concrete on IAQ and indoor RH has modelled and investigated. Two similarity coefficients $\kappa_{K_m,VOC}$ and $\kappa_{\mu,VOC}$ defined for VOC storage and diffusion have been proposed and can be used to estimate the VOC properties from the vapor diffusion resistance factor ($\mu_{m,wv}$) and the slope of the sorption curve in the monolayer sorption range of the same material. The toluene properties ($K_{m,TOL}$ and $D_{m,TOL}$) were determined from the hygric properties of hemp concrete

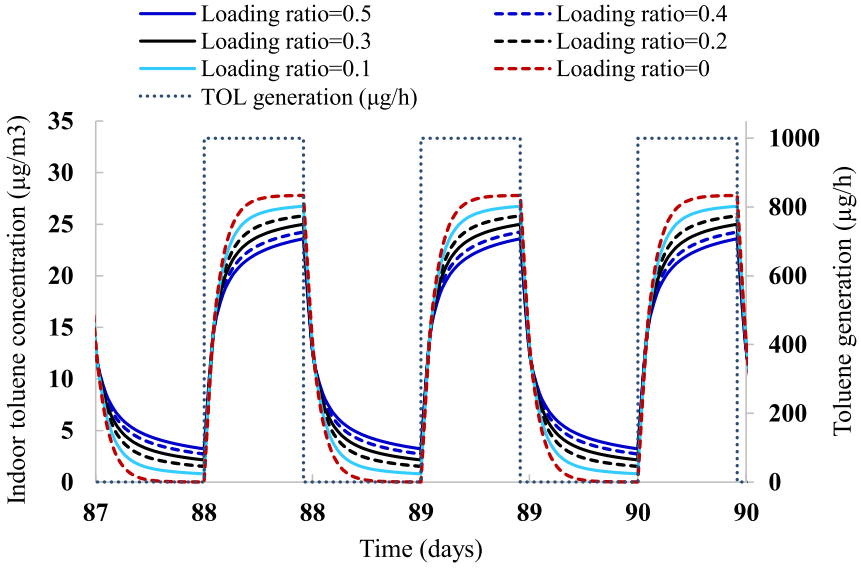

Fig. 12. Effect of loading ratio (m^2/m^3) of hemp concrete on indoor toluene concentration.

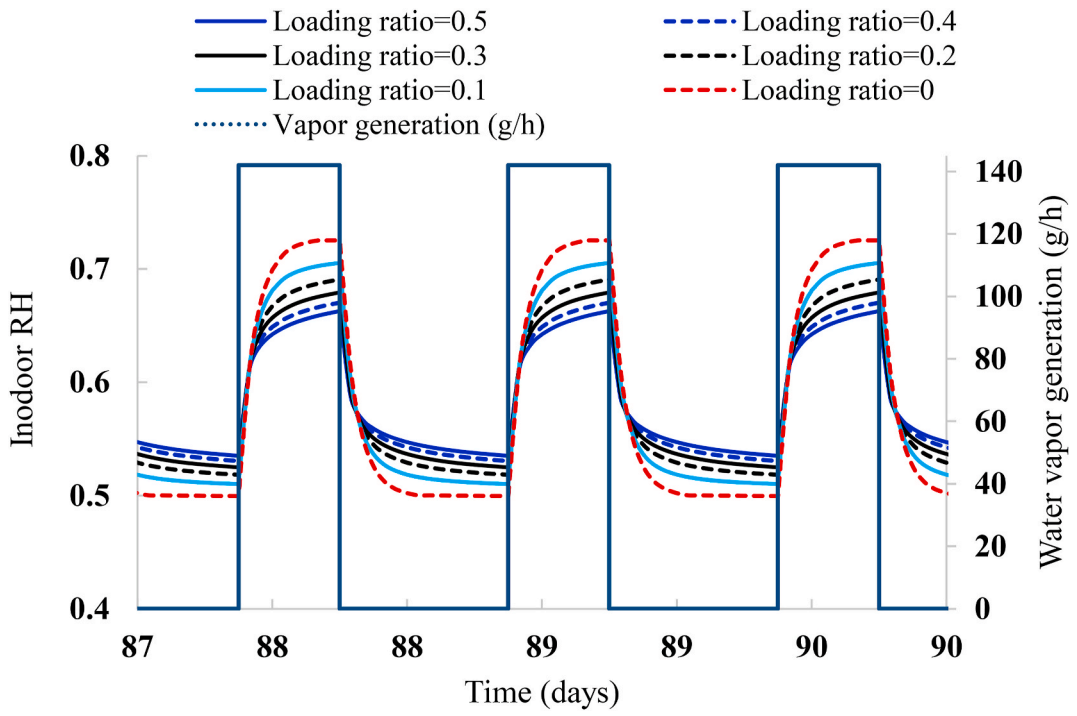

Fig. 13. Effect of loading ratio (m^2/m^3) of hemp concrete on indoor RH.

Table 7
Impact of exposed surface (A) and loading ratio on toluene performance of hemp concrete.

A (m^2)	Loading ratio A/V (m^2/m^3)	C_{max} ($\mu g/m^3$)	C_{min} ($\mu g/m^3$)	Amplitude ($\mu g/m^3$)	PRF_{TOL} (%)	$ERF_{c,TOL}$ (%.h)
0	0.0	27.8	0.0	27.8	0.0	0.0
5	0.1	26.8	0.8	25.9	3.7	56.0
10	0.2	25.8	1.5	24.3	7.1	103.9
15	0.3	25.0	2.1	22.9	10.0	144.5
20	0.4	24.3	2.7	21.6	12.6	179.7
25[a]	***0.5***	***23.6***	***3.2***	***20.4***	***15.0***	***210.5***

[a] Reference case.

Table 8
Impact of exposed surface (A) and loading ratio on hygric performance of hemp concrete.

A (m^2)	Loading ratio S/V (m^2/m^3)	RH_{max} (%)	RH_{min} (%)	Amplitude (%)	RF_a (%)	PRF_{RH} (%)
0	0.00	72.5	50	22.5	0.0	0.0
5	0.10	70.5	51.0	19.5	13.6	2.8
10	0.20	69.1	51.8	17.3	23.7	4.8
15	0.30	67.9	52.5	15.5	31.6	6.4
20	0.40	67.0	53.0	14.0	38.1	7.6
25[a]	**0.50**	**66.3**	**53.5**	**12.8**	**43.4**	**8.6**

[a] Reference case.

based on the assumption of the similarity between the moisture and pollutant transport in porous materials. The coupled moisture and pollutant transport simulation model has been established and implemented in SPARK, an object-oriented program suited to complex problems. The numerical model was applied to investigate the effect of the toluene and moisture buffering capacities of hemp concrete on indoor toluene concentration and relative humidity. The results reveal that taking into account the sorption capacity toward moisture and toluene of hemp concrete has a significant impact on indoor RH and IAQ. Numerically, in this case studied, hemp concrete can contribute to dampen 15% the peark of indoor toluene concentration and 43.4% indoor RH variation amplitude. The indices are also proposed to represent the buffering capacity of materials in reducing the occupant's peak exposure (RH and toluene), cumulative exposure to toluene. These definitions are very useful for consideration in future standards that consider buffering as an approach to improving IAQ as well as hygrothermal performance of buildings. Further experiments and analyses are needed to generalize the similarity and the potential of VOC and moisture buffering capacities of bio-based materials for other VOCs with different physical properties (size, molar mass, polarity, etc.). Finally, it is important to note that the developed numerical model allows to study quantitatively the effect of different parameters (D_m, $K_{m,\ VOC}$, exposed surface, loading ratio, etc.) on the IAQ and thermal comfort and can be used to predict the entire VOC emission life of the material to overcome the measurement difficulties.

Declaration of competing interest

We wish to confirm that there are no known conflicts of interest associated with this publication and there has been no significant financial support for this work that could have influenced its outcome.

Acknowledgements

This study was carried out under the program Fulbright/Hauts-de-France which is supported by the Franco-American Fulbright Commission and the Hauts-de-France region, France. Thanks to this financial support, it enabled Dr. Anh Dung TRAN LE to work at the BEESL of Syracuse University, USA for a period of six months. The authors wish to thank them.

The authors wish to thank the editor and reviewers for their constructive and useful comments on the previous version of this article.

Nomenclature

A	Exposed area of the material m^2
C	Concentration kg/m^3
$C_{a,o}$	Outdoor ventilation air kg/m^3
$C_{a,wv,e}$	Water vapor concentrations in the outside kg/m^3
$C_{a,wv,i}$	Water vapor concentrations in the room air kg/m^3
$D_{m,VOC}$	Diffusion coefficient of the VOC in the material $m^2.s^{-1}$
$D_{m,wv}$	Mass transport coefficient associated to a moisture content gradient $m^2.s^{-1}$
D_{VOC}^{air}	VOC diffusion coefficient in the free air m^2/s
D_{wv}^{air}	Water vapor diffusion coefficient in the free air m^2/s
$h_{m,wv,i}$	Convective water vapor transfer coefficient for the internal surface m/s
$h_{m,wv,e}$	Convective water vapor transfer coefficient for the external surface m/s
$h_{m,VOC,e}$	Convective VOC transfer coefficient for the external surface m/s
$h_{m,VOC,i}$	Convective VOC transfer coefficient for the internal surface m/s
$K_{m,VOC}$	Partition coefficient for VOC
$K_{m,wv}$	Partition coefficient for water vapor
ERFc	Cumulative Exposure Reduction Factor %.h
PRF	Peak reduced factor %
$P_{wv,sat}$	Saturation pressure of water vapor Pa
Q	Flow rate m^3/s
RH	Relative humidity
R_v	Gas constant for water vapor J/(kg·K)
T	Temperature K
t	Time s
V	Volume space m^3
w	Moisture content $kg.kg^{-1}$
w_m	Monolayer moisture content $kg.kg^{-1}$
x	Abscissa m
θ	Moisture volumetric content $m^3.m^{-3}$
μ_{wv}	Vapor diffusion resistance factor
δ_{wv}	Water vapor permeability of material kg/(m.s.Pa)
δ_{wv}^{a}	Water vapor permeability of still air kg/(m.s.Pa)
$\kappa_{\mu,VOC}$	Similarity coefficient for the moisture and VOC diffusion
$\kappa_{K_m,VOC}$	Similarity coefficient for the moisture and VOC storage

Subscripts

e	external
m	material
i	internal
wv	water vapor
VOC	Volatile Organic Compounds

References

[1] S. Hameury, Moisture buffering capacity of heavy timber structures directly exposed to an indoor climate: a numerical study, Build. Environ. 40 (10) (2005) 1400–1412.

[2] M. Woloszyn, T. Kalamees, M.O. Abadie, M. Steeman, A.S. Kalagasidis, The effect of combining a relative-humidity-sensitive ventilation system with the moisture-buffering capacity of materials on indoor climate and energy efficiency of buildings, Build. Environ. 44 (2009) 515–524.

[3] A.D. Tran Le, C. Maalouf, T.H. Mai, E. Wurtz, F. Collet, Transient hygrothermal behaviour of a hemp concrete building envelope, Energy Build. 42 (2010) 1797–1806.

[4] D. Samri, Analyse physique et caractérisation hygrothermique des matériaux de construction : approche expérimentale et modélisation numérique, Thèse ENTPE de Lyon, France, 2006.

[5] A.D. Tran Le, C. Maalouf, O. Douzane, G. Promis, T.H. Mai, T. Langlet, Impact of combined the moisture buffering capacity of a hemp concrete building envelope and interior objects on the hygrothermal comfort in a building, Journal of Building Performance Simulation 9 (6) (2016) 589–605.

[6] B. Moujalled, Y.A. Oumeziane, S. Moissette, M. Bart, C. Lanos, D. Samri, Experimental and numerical evaluation of the hygrothermal performance of a hemp lime concrete building: a long term case study, Build. Environ. 136 (2018) 11–27, https://doi.org/10.1016/j.buildenv.2018.03.025.

[7] D. Maskell, C.F. Da Silva, K. Mower, R. Cheta, A. Dengel, R. Ball, M. Ansell, P. Walker, A. Shea, Properties of bio-based insulation materials and their potential impact on indoor air quality, in: First International Conference on Bio-Based Building Materials, 2015, 2015.

[8] F.P. Da SilvaCarla, R. Chetas, M. Daniel, D. Andy, P. Ansell Martin, J. Ball Richard, Influence of eco-materials on indoor air quality, Green Mater. 4 (2) (2016) 72–80, 2016.

[9] J. Gunschera, S. Mentese, T. Salthammer, J.R. Andersen, Impact of building materials on indoor formaldehyde levels: effect of ceiling tiles, mineral fiber insulation and gypsum board, Build. Environ. 64 (2013) 138–145.

[10] X. Li, R. Xiao, J.J. Morrell, X. Zhou, G. Du, Improving the performance of hemp hurd/polypropylene composites using pectinase pre-treatments, Ind. Crop. Prod. 97 (2017) 465–468, https://doi.org/10.1016/j.indcrop.2016.12.061.

[11] E. Gourlay, P. Glé, S. Marceau, C. Foy, S. Moscardelli, Effect of water content on the acoustical and thermal properties of hemp concretes, Construct. Build. Mater. 139 (2017) 513–523.

[12] S. Amziane, F. Collet, M. Lawrence, C. Magniont, V. Picandet, M. Sonebi, Recommendation of the RILEM TC 236-BBM: characterisation testing of hemp shiv to determine the initial water content, water absorption, dry density, particle size distribution and thermal conductivity, Mater. Struct. 50 (2017) 167.

[13] M. Lagouin, C. Magniont, P. Sénéchal, P. Moonen, J.-E. Aubert, L. Aurélie-préneron, Influence of types of binder and plant aggregates on hygrothermal and mechanical properties of vegetal concretes, Construct. Build. Mater. 222 (2019) 852–871.

[14] T. Adamová, J. Hradecký, M. Prajer, VOC emissions from spruce strands and hemp shive: in search for a low emission raw material for bio-based construction materials, *Materials* (Basel) 12 (12) (2019) 2026, https://doi.org/10.3390/ma12122026. PMID: 31238573; PMCID: PMC6630300.

[15] M. Viel, F. Collet, Y. Lecieux, M.L.M. François, V. Colson, C. Lanos, A. Hussain, M. Lawrence, Resistance to mold development assessment of bio-based building materials, Compos. B Eng. 158 (2019) 406–418.

[16] Y. Aït Oumeziane, F. Collet, C. Lanos, B. Moujalled, Modelling the hygrothermal behaviour of hemp concrete: from material to building, in: G. Crini, E. Lichtfouse (Eds.), Sustainable Agriculture Reviews 42, Sustainable Agriculture Reviews, vol. 42, Springer, Cham, 2020.
[17] X. Li, S. Wang, G. Du, Z. Wu, Y. Meng, Variation in physical and mechanical properties of hemp stalk fibers along height of stem, Ind. Crop. Prod. 42 (2013) 344–348.
[18] M. Koivula, H.-R. Kymäläinen, J. Virta, et al., Emissions from thermal insulations–part 2: evaluation of emissions from organic and inorganic insulations, Build. Environ. 40 (2005) 803–814.
[19] F. Collet, M. Bart, L. Serres, J. Miriel, Porous structure and water vapour sorption of hemp-based materials, Construct. Build. Mater. 22 (2008) 1271–1280.
[20] R. Walker, S. Pavía, Moisture transfer and thermal properties of hemp–lime concretes, Construct. Build. Mater. 64 (2014) 270–276.
[21] D. Lelievre, Simulation numérique des transferts de chaleur et d'humidité dans une paroi multicouche de bâtiment en matériaux biosourcés, Université Bretagne-Sud, 2015.
[22] M. Rahim, O. Douzane, A.D. Tran Le, G. Promis, B. Laidoudi, A. Crigny, et al., Characterization of flax lime and hemp lime concretes: hygric properties and moisture buffer capacity, Energy Build. 88 (2015) 91–99.
[23] T. Colinart, P. Glouannec, Temperature dependence of sorption isotherm ofhygroscopic building materials. Part 1: experimental evidence and modeling, Energy Build. 139 (2017) 360–370.
[24] G. Promis, L.F. Dutra, O. Douzane, A.D. Tran Le, T. Langlet, Temperature-dependent sorption models for mass transfer throughout bio-based building materials, Construct. Build. Mater. 197 (2019) 513–525.
[25] T.T. Nguyen, V. Picandet, S. Amziane, C. Baley, Influence of compactness and hemp hurd characteristics on the mechanical properties of lime and hemp concrete, European Journal of Environmental and Civil Engineering 13 (9) (2009) 1039–1050.
[26] C. Magniont, G. Escadeillas, M. Coutand, C. Oms-Multon, Use of plant aggregates in building ecomaterials, Eur. J. Environ. Civil Eng. 16 (2012) s17.
[27] J. Williams, M. Lawrence, P. Walker, The influence of the casting process on the internal structure and physical properties of hemp-lime, Mater. Struct. 50 (2) (2017) 108.
[28] A.D. Tran Le, S.T. Nguyen, T. Langlet, A novel anisotropic analytical model for effective thermal conductivity tensor of dry lime-hemp concrete with preferred spatial distributions, Energy Build. 182 (2019) 75–87.
[29] M. Salonvaara, J.S. Zhang, M. Yang, A study of air, water and VOC transport through building materials with the dual chamber system, in: Proc. Of Int. Specialty Conf.: *Indoor Environmental Quality – Problems*, Research and Solutions, *Durham*, NC, 2006.
[30] J. Xu, J. Zhang, J. Grunewald, J. Zhao, R. Plagge, Q. Amiri, et al., A study on the similarities between water vapor and VOC diffusion in porous media by a dual chamber method, Clean 37 (6) (2009) 444–453.
[31] C. Rode, J. Grunewald, L. Liu, M. Qin, J. Zhang, Models for residential indoor pollution loads due to material emissions under dynamic temperature and humidity conditions, 12th Nordic Symposium on Building Physics (NSB 2020) (2020), 11002, https://doi.org/10.1051/e3sconf/202017211002, 2020.
[32] X. Yang, Q. Chen, J.S. Zhang, R. Magee, J. Zeng, C.Y. Shaw, Numerical simulation of VOC emissions from dry materials, Build. Environ. 36 (10) (2001) 1099–1107.
[33] H. Huang, F. Haghighat, Modelling of volatile organic compounds emission from dry building materials, Build. Environ. 37 (2002) 1127–1138.
[34] J.S. Zhang, Combined heat, air, moisture, and pollutants transport in building environmental systems, *JSME International Journal*, Series B 48 (2) (2005) 1–9.
[35] J.R. Philip, D.A. De Vries, Moisture movement in porous materials under temperature gradients, Trans. Am. Geophys. Union 38 (2) (1957) 222–232.
[37] P.R.D. Andrade, M.R. Lemus, C.C.E. Pérez, Models of sorption isotherms for food: uses and limitations, Vitae 18 (2011) 325–334.
[38] J.W. Axley, Adsorption modelling for building contaminant dispersal analysis', Indoor Air 1 (2) (1991) 147–171.
[39] P. Blondeau, A.L. Tiffonnet, F. Allard, F. Highighat, Physically based modeling of the material and gaseous contaminant interactions in buildings: models, experimental data and future developments, Adv. Build. Energy Res. 2 (1) (2008) 57–93, https://doi.org/10.3763/aber.2008.0203.
[40] F.M. White, Heat and Mass Transfer, Addison-Wesley, New York, 1991.
[41] E.F. Sowell, P. Haves, Efficient solution strategies for building energy system simulation, Energy Build. 33 (2001) 309–317.
[42] E. Wurtz, F. Haghighat, L. Mora, K.C. Mendonca, C. Maalouf, H. Zhao, P. Bourdoukan, An integrated zonal model to predict transient indoor humidity distribution, Build. Eng. 112 (2) (2006) 175–186.
[43] K.C. Mendonça, C. Inard, E. Wurtz, F.C. Winkelmann, F. Allard, A zonal model for predicting simultaneous heat and moisture transfer in buildings, in: Indoor Air 2002, 9th International Conference on Indoor Air Quality and Climate, 2002.
[44] A.D. Tran le, C. Maalouf, K.C. Mendonça, T.H. Mai, E. Wurtz, Study of moisture transfer in doubled-layered wall with imperfect thermal and hydraulic contact resistances, Journal of Building Performance Simulation (2) (2009) 251–266.
[45] Jing Xu, J.S. Zhang, An experimental study of relative humidity effect on VOCs' effective diffusion coefficient and partition coefficient in a porous medium, Build. Environ. 46 (9) (2011) 1785–1796.
[46] F. Collet, J. Chamoin, S. Pretot, C. Lanos, Comparison of the hygric behaviour of three hemp concretes, Energy Build. 62 (2013) 294–303.
[47] F. Collet, Caractérisation hydrique et thermique de matériaux de génie civil à faibles impacts environnementaux, Thèse de Doctorat, 2004. INSA de Rennes.
[48] A. Bodalal, Fundamental Mass Transfer Modeling of Emission of Volatile Organic Compounds from Building Materials, PhD thesis, Department of Mechanical and Aerospace Engineering, Carleton, University, Canada, 1999.
[49] E. Latif, M. Lawrence, A. Shea, P. Walker, Moisture buffer potential of experimental wall assemblies incorporating formulated hemp-lime, Build. Environ. 93 (2) (2015) 199–209, 2015.
[53] A Shea, M Lawrence, P Walker, Hygrothermal performance of an experimental hemp–lime building, Construct. Build. Mater. 36 (2012) 270–275.
[54] F.O Olalekan, C.J Simonson, Moisture buffering capacity of hygroscopic building materials: Experimental facilities and energy impact, Energy Build. 38 (2006) 1270–1282.
[55] E Hunter-Sellars, J.J Tee, P I Parkin, D.R Williams, Adsorption of volatile organic compounds by industrial porous materials: Impact of relative humidity, Microporous Mesoporous Mater. 298 (2020), 110090, https://doi.org/10.1016/j.micromeso.2020.110090.
[56] T G Matthews, A R Hawthorne, C V Thompson, Formaldehyde sorption and desorption characteristics of gypsum wallboard, Environ. Sci. Technol. 21 (7) (1987) 629–634, https://doi.org/10.1021/es00161a002.
[57] B C Singer, K L Revzan, T Hotchi, A T Hodgson, N J Brown, Sorption of organic gases in a furnished room, Atmos. Environ. 38 (16) (2004) 2483–2494, https://doi.org/10.1016/j.atmosenv.2004.02.003.
[58] P Promis, O Douzane, A.D Tran Le, T Langlet, Moisture hysteresis influence on mass transfer through bio-based building materials in dynamic state, Energy Build. 166 (1) (2018) 450–459.
[59] P Crausse, J.P Laurent, B Perrin, Influence des phénomènes d'hystérésis sur les propriétés hydriques de matériaux poreux: Comparaison de deux modèles de simulation du comportement thermohydrique de parois de bâtiment, Revue Générale de Thermique 35 (410) (1996) 95–106, https://doi.org/10.1016/S0035-3159.
[60] E O Timmermann, Multilayer sorption parameters: BET or GAB values? Colloids Surf A Physicochem. Eng. Asp. 220 (2003) 235–260.
[61] I Langmuir, The adsorption of gases on plane surfaces of glass, mica and platinum, J. Am. Chem. Soc. 40 (9) (1981) 1361–1403.
[62] S Brunauer, P Emmet, E Teller, Adsorption of gases in multimolecular layers, J. Am. Chem. Soc. 60 (2) (1938) 309–319.
[63] Y A Cengel, A J Ghajar. Heat and mass transfer: fundamentals and applications, 4th ed, McGraw-Hill, New York, 2010.
[64] K Zu, M Qin, C Rode, M Libralato, Development of a moisture buffer value model (MBM) for indoor moisture prediction, Appl. Therm. Eng. (2020), 115096, https://doi.org/10.1016/j.applthermaleng.2020.115096.